JOURNAL OF GEOPHYSICAL RESEARCH, VOL. 97, NO. D9, PAGES 10,103–10,108, JUNE 20, 1992

Polynomial Coefficients for Calculating O_2 Schumann-Runge Cross Sections at 0.5 cm^{-1} Resolution

K. MINSCHWANER

Department of Earth and Planetary Sciences, Harvard University, Cambridge, Massachusetts

G. P. ANDERSON AND L. A. HALL

Phillips Laboratory, Geophysics Directorate ,Hanscom Air Force Base, Bedford, Massachusetts

K. YOSHINO

Harvard-Smithsonian Center for Astrophysics, Cambridge, Massachusetts

We have fitted O_2 cross sections from 49,000 to 57,000 cm^{-1} with temperature dependent polynomial expressions, providing an accurate and efficient means of determining Schumann-Runge band cross sections for temperatures 130<T<500 K. The least squares fits were carried out on a 0.5 cm^{-1} spectral grid, using cross sections obtained from a Schumann-Runge line-by-line model that incorporates the most recent spectroscopic data. The O_2 cross sections do not include the underlying Herzberg continuum, but they do contain contributions from the temperature dependent Schumann-Runge continuum. The cross sections are suitable for use in ultraviolet transmission calculations at high spectral resolution. They should also prove useful for updating existing parameterizations of ultraviolet transmission and O_2 photolysis.

1. INTRODUCTION

Terrestrial absorption of solar radiation between 175 and 205 nm plays a key role in the photochemistry of the middle atmosphere. Photodissociation of O_2 in this spectral region is the dominant source of odd oxygen in the mesosphere, and the transmission of 175-205 nm solar radiation regulates the photodissociation rates of stratospheric H_2O, NO, N_2O, and a variety of CFC molecules. Opacity in this wavelength interval is dominated by the Schumann-Runge (S-R) bands of oxygen, a dense spectral progression containing thousands of overlapping lines. Owing to this complexity, O_2 absorption in the S-R bands has long posed problems for modeling the photochemistry of the middle atmosphere (see, for example, *World Meteorological Organization (WMO)* [1986]). Mean-band parameterizations often have been employed to approximate S-R band absorption over relatively wide spectral intervals. In this regard, previous studies were successful in developing an understanding of the photochemical implications of ultraviolet absorption in the S-R bands [*Park*, 1974; *Fang et al.*, 1974; *Nicolet and Peetermans*, 1980; *Allen and Frederick*, 1982]. However, quantitative assessment was impeded by insufficient resolution in laboratory measurements of O_2 cross sections [*Brix and Herzberg*, 1954; *Hudson and Carter*, 1968; *Ackerman et al.*, 1970].

Recent measurements provide high resolution, absolute oxygen cross sections between 175 and 205 nm, at temperatures of 300 and 79 K [*Yoshino et al.*, 1983, 1987]. The calculations of *Murtagh* [1988] and *Nicolet and Kennes* [1989] incorporated the new spectroscopic data into mean-band models for ultraviolet transmission and O_2 photolysis. While band parameterizations are useful for specific applications to atmospheric modeling, it was felt that a broader purpose could be served by providing the means to represent S-R band cross sections at high spectral resolution, over a range of atmospheric temperatures. A reevaluation of O_2 absorption in the S-R bands, in light of the new laboratory data, is clearly warranted.

We describe a new line-by-line code which permits calculation of O_2 S-R cross sections at arbitrary spectral resolution and temperature. Procedures are outlined for fitting polynomial expressions to the temperature dependence of these cross sections on a 0.5 cm^{-1} spectral grid. It is demonstrated that the polynomial-generated cross sections are well suited for atmospheric transmission calculations at high spectral resolution.

2. SCHUMANN-RUNGE LINE-BY-LINE ALGORITHM

The magnitude of the S-R cross section is determined in the line-by-line model by a sum of contributions from each spectral line lying within a predetermined spectral interval. The quantities required to perform this calculation are the position, strength, and half width of each spectral line. Measured spectroscopic constants of the $B^3\Sigma_u^-$ and $X^3\Sigma_g^-$ electronic states of O_2 [*Veseth and Lofthus*, 1974; *Cheung et al.*, 1986*a*] are used to calculate energies of the vibrational and spin-split rotational levels and to determine line positions. The model includes spectral lines from 14 branches (six principal, six satellite, and two forbidden) for bands with $v'=0$ to 19, and $v''=0$ to 2, including rotational levels $N''=1$ to 51. We use the conventional notation here for the lower state ($X^3\Sigma_g^-$) vibrational quantum number, v'', total angular momentum excluding spin, N'', and upper state ($B^3\Sigma_u^-$) vibrational level, v'. Mean band oscillator strengths are adopted from *Yoshino et al.* [1987] and *Lewis et al.* [1986*a*], and rotationally dependent Hönl-London factors are obtained from *Tatum and Watson* [1971]. Predissociation widths, including their dependence on rotational levels, are taken

Paper number 92JD00661
0148-0227/92/92JD-00661$05.00

from *Cheung et al.* [1990] and *Lewis et al.* [1986*b*]. The effects of the S-R bands of $^{16}O^{18}O$ (0.41% of atmospheric O_2) are incorporated into the model, based on spectroscopic parameters of *Cheung et al.* [1989], *Yoshino et al.* [1989], and *Chiu et al.* [1990]. The model includes more than 10,000 lines in the wavelength interval 175-205 nm.

The temperature dependence of line strengths is calculated explicitly through the Boltzmann population distribution. Temperature also enters into the calculation through Doppler broadening of line profiles. Accordingly, a full Voigt line profile is used [*Drayson*, 1976], containing both a Lorentzian contribution from predissociation broadening and a Gaussian component from Doppler broadening. A detailed analysis showed that 0.5 cm^{-1} resolution was sufficient to capture most of the fine structure of S-R cross sections; we thus employ a 16,000 point spectral grid covering range 49,000 to 57,000 cm^{-1}. Since the wings of distant spectral lines create a quasi-continuum in the window regions, we consider the contribution from all lines that lie within 500 cm^{-1} from each spectral point.

The underlying Herzberg continuum is not included in our model cross sections. This decision was motivated by two factors: first, the Herzberg pressure dependence [*Cheung et al.*, 1986*b*] is not easily incorporated into our formulation (although this effect is negligible in the middle atmosphere); second, since there is still debate over the magnitude of the Herzberg contribution in the S-R band region [*DeMore et al.*, 1990], the option exists to choose among various analytic expressions in the literature [e.g., *Nicolet and Kennes*, 1986; *Yoshino et al.*, 1988; *Yoshino et al.*, 1992]. Absorption by the underlying S-R continuum is, however, included in the model. The cross sections for the S-R continuum are based on the formulation of *Lewis et al.* [1985*a*], where the temperature dependence is found by summing over all Boltzmann-weighted partial cross sections. An additional contribution to the continuum by transitions into the $^3\Pi_g$ state is accounted for by an empirical fit to the results of *Lewis et al.* [1985*b*] at 80 K.

Agreement between the model and the laboratory values of the O_2 cross section is exceptionally good for both 79 and 300 K, over the entire spectral range. The agreement is also satisfactory at much higher temperatures (~ 500 K), based on comparisons with unpublished measurements from the Harvard-Smithsonian Center for Astrophysics. Figures 1*a*-1*c* illustrate the level of agreement between the model and the observations at temperatures of 79 K [*Yoshino et al.*, 1987], 300 K [*Yoshino et al.*, 1987], and 505 K. The model accurately reproduces the measured cross sections at these temperatures, lending confidence to its utility over the range of atmospheric temperatures normally encountered in the stratosphere, mesosphere, and lower thermosphere.

3. TEMPERATURE DEPENDENCE

As mentioned previously, the temperature dependence of Schumann-Runge cross sections results from changes both in the Boltzmann population distribution and in the Doppler line widths, but since predissociation widths typically exceed Doppler widths by a factor of 10 or more, the Boltzmann effect is much more dominant. The fractional population of a particular energy state is given by

$$F(v'',N'') = \frac{(2N''+1)\exp\left[-\dfrac{hcE(v'',N'')}{kT}\right]}{\sum_{v''}\sum_{N''}(2N''+1)\exp\left[-\dfrac{hcE(v'',N'')}{kT}\right]} \quad (1)$$

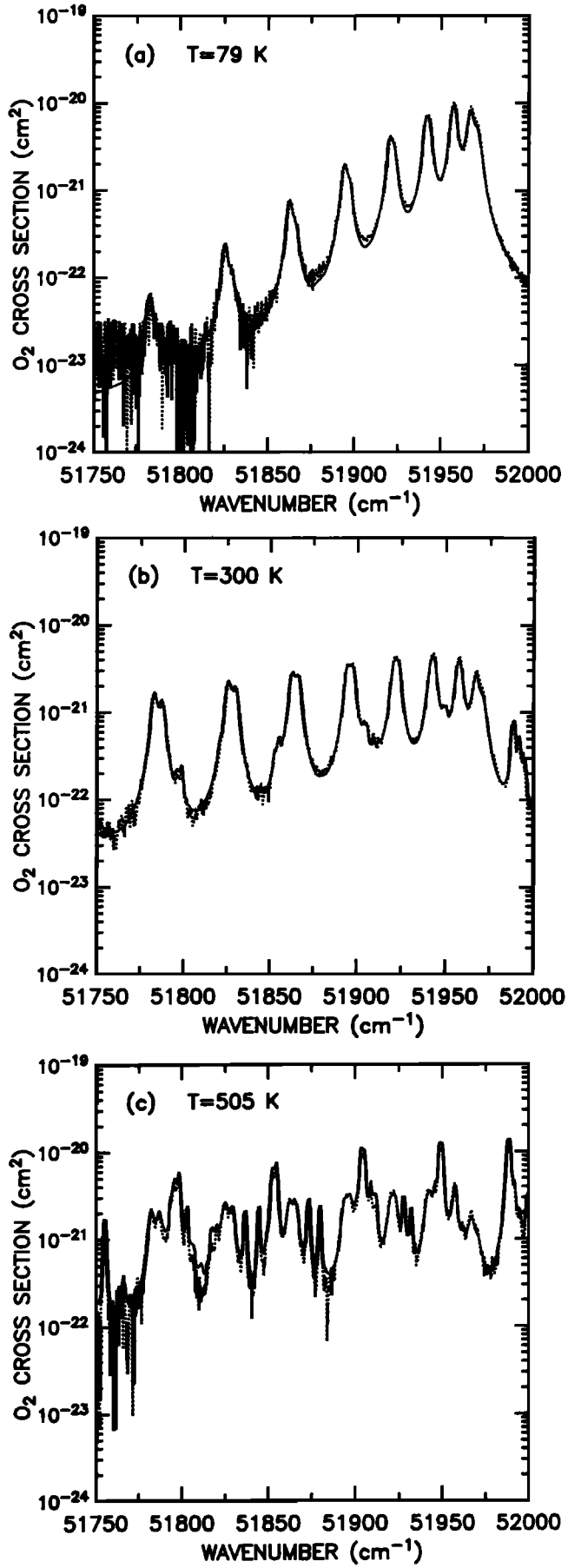

Fig. 1. Model S-R cross sections (solid) and measured cross sections (dotted) from the Harvard-Smithsonian laboratory at (*a*) 79 K, (*b*) 300 K, and (*c*) 505 K.

where h and k are the Planck and Boltzmann constants, c is the vacuum speed of light, E is the state energy, and T is the temperature. Since line strengths vary in direct proportion to the fractional population of the lower state, the behavior of S-R cross sections with changes in temperature is intimately connected to the lower state energy of spectral lines. As an example of this temperature dependence, Figure 2 shows S-R band cross sections from 55,420 to 55,470 cm^{-1}, at temperatures ranging from 130 to 500 K. It can be seen that cross sections near $v''=0$ band heads (N'' less than about 5, or relatively small lower state energies) decrease as the temperature is raised from 130 K. Conversely, cross sections near lines originating from higher vibrational levels, or ground vibrational levels with a large value of N'' (corresponding to comparatively larger lower state energies), generally increase with rising temperature. Figure 3 displays the temperature dependence at four spectral locations, where three of these correspond to cross sections shown in Figure 2. The behavior of cross sections at 55,454 and 52,738 cm^{-1} is particularly difficult to characterize analytically, although qualitatively the interpretation is straightforward. For example, at 55,454 cm^{-1} the low-temperature cross section is controlled by the contribution from the wings of the 11-0 band head; thus as the temperature increases, the cross section initially decreases. However, at about 200 K the $v''=1$ states become sufficiently populated to allow the emergence of the 19-1 band in this region, which quickly dominates the decaying 11-0 lines as the temperature increases further.

In light of the above discussion we should expect that the most natural fitting procedure would involve the sum of exponential functions:

$$\sigma(\nu,T) = \left[\frac{A(\nu)}{T}\right] e^{\frac{-B(\nu)}{T}} + \left[\frac{C(\nu)}{T}\right] e^{\frac{-D(\nu)}{T}} + \cdots \quad (2)$$

where σ is the fitted cross section and the coefficients A, B, C, and D are determined from the model cross section at each wavenumber ν. It is easy to show that the individual terms in equation (2) arise from the temperature dependence of line strengths; each term represents a contribution to the cross section by a nearby line, and the value of the cross section is typically determined by one or two local lines. Although this description can be defended on theoretical grounds, a fitting method which is linear with respect to the fit coefficients is much easier to implement in a discrete layer atmospheric model. This can be seen through the expression for Beer's law absorption

$$\tau_j(\nu) = \exp\left[-\sum_{i=j}^{N}\sigma(\nu,T_i)N_i\right] \quad (3)$$

where $\tau_j(\nu)$ is the transmission at level j, N_i is the slant column density of O_2 in the i^{th} atmospheric layer, and the summation extends over all layers above level j. If the cross section is expressed as a linear combination of basis functions f(T), g(T), and h(T), for example,

$$\sigma(\nu,T) = A(\nu)f(T) + B(\nu)g(T) + C(\nu)h(T) \quad (4)$$

then equation (3) may be rewritten as

$$\tau_j(\nu) = \exp\left[-A(\nu)\sum_{i=j}^{N}f(T_i)N_i - B(\nu)\sum_{i=j}^{N}g(T_i)N_i - C(\nu)\sum_{i=j}^{N}h(T_i)N_i\right] \quad (5)$$

The above sums, representing temperature-weighted column amounts, are independent of ν and only need to be computed once for a given temperature profile, saving a considerable amount of computational expense for calculations requiring additional integrations over ν. The efficiency of a similar formulation has been demonstrated for calculations using the temperature dependent Hartley-Huggins ozone absorption cross sections of *Bass and Paur* [1985] (see, for example, atmospheric radiance codes such as LOWTRAN 7 [*Kneizys et al.*, 1988; *Anderson et al.*, 1990]).

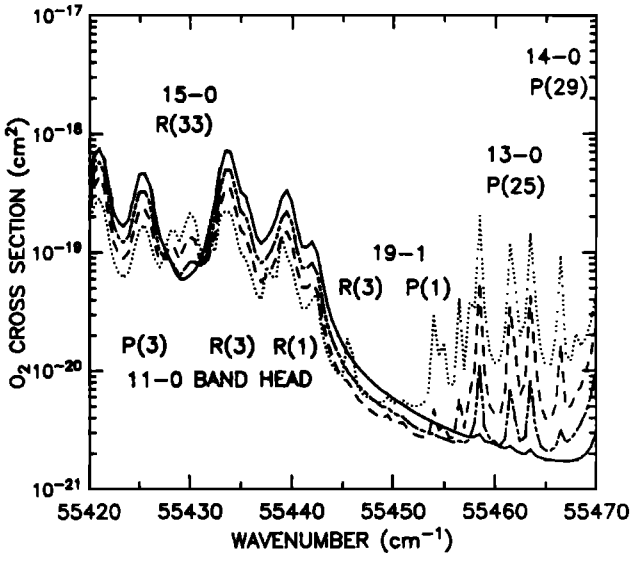

Fig. 2. Model S-R cross sections at 130 K (solid), 200 K (solid-dashed), 300 K (dashed), and 500 K (dotted). Note that cross sections near the 11–0 band head decrease with increasing temperature, while cross sections near high–N'' lines of the 13–0, 14–0, and 15-0 bands become larger with increasing temperature. Cross sections near lines of the 19–1 band are also larger at higher temperatures.

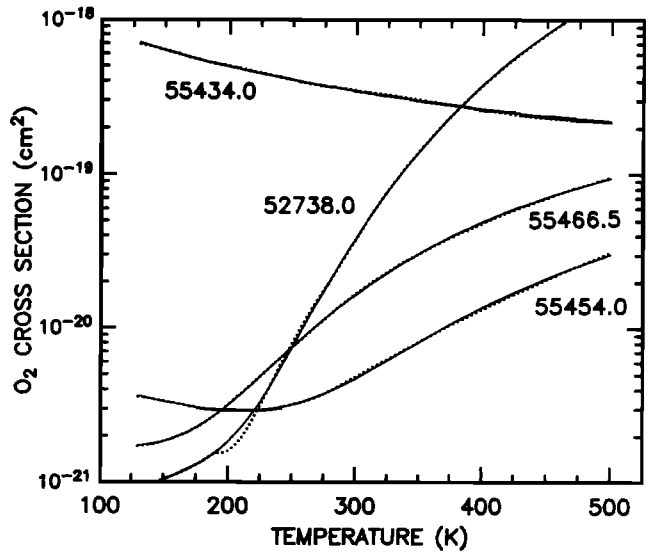

Fig. 3. Temperature dependence of S-R cross sections at 55434.0, 55454.0, 55466.5, and 52738.0 cm^{-1} (the cross section at 52738.0 cm^{-1} has been multiplied by a factor of 100). The dotted curves are polynomial fits to the cross sections obtained by procedures outlined in the text.

The quadratic polynomial used by Bass and Paur for ozone ($aT^2 + bT + c$) proved inadequate to describe the S-R band temperature dependence. Considerable difficulty was encountered at many spectral points due to a weak dependence at low temperature, compounded by a rapid growth observed at higher temperatures. Furthermore, the temperature dependence often exhibited changes in the sign of the curvature (compare Figure 3) typically arising from a superposition of terms representing contributions from different spectral lines. A function composed of the even terms of a quartic polynomial was found to adequately simulate this behavior, provided that the temperature variable was transformed according to

$$\Delta = \left[\frac{T-100}{10}\right]^2 \tag{6}$$

The fit function thus takes the form

$$\sigma(\nu,T) = A(\nu)\Delta^2 + B(\nu)\Delta + C(\nu) \tag{7}$$

where $A(\nu)$, $B(\nu)$ and $C(\nu)$ are the fitted coefficients at each wavenumber. Equation (7) describes a quartic polynomial in temperature which is symmetric about an axis defined by T=100 K, so that $d\sigma/dT = 0$ at 100 K. The fit function thus has the capacity to simulate the flat behavior observed at low temperatures, while retaining the advantages of a higher-order polynomial in order to capture the nearly exponential dependence, including points of inflection, which was observed at higher temperatures.

The integrity of the fit was constrained in some cases, however, to a temperature range of only $\Delta T \sim 50$ K. Since our objective was to include the range of atmospheric temperatures normally encountered over altitudes from 0 to 120 km (~ 130 to 500 K), we adopted a piecewise continuous fit over three distinct temperature intervals

$$\sigma(\nu,T) = \begin{cases} A_1(\nu)\Delta^2 + B_1(\nu)\Delta + C_1(\nu) & 130 < T \le 190 \\ A_2(\nu)\Delta^2 + B_2(\nu)\Delta + C_2(\nu) & 190 < T \le 280 \\ A_3(\nu)\Delta^2 + B_3(\nu)\Delta + C_3(\nu) & 280 < T \le 500 \end{cases} \tag{8}$$

Although the formulation described by equation (8) requires that only atmospheric layers within the same temperature regime, as defined above, can be grouped together into a temperature-weighted column amount, viz., equation (5), there is still a substantial computational savings in implementing the linear (with respect to fitted coefficients) representation.

The coefficients were determined using a least squares fitting procedure, with the fits constrained to match the line-by-line results at boundaries between temperature intervals. The boundaries were chosen to provide the best compromise in fitting errors between adjacent temperature intervals. In many cases the boundaries corresponded to locations where the cross section exhibited a relatively abrupt change in behavior with respect to temperature due to the emergence of hot ($v''>0$) lines.

The largest fitting errors were encountered at low temperatures, within the spectral range 49,000-50,000 cm^{-1}. Under these conditions the S-R band cross section contains relatively deep windows between band heads due to the absence of high-N'' lines. Figure 4*a* shows the magnitude of the maximum error in the fit for the temperature range 190-280 K. Nearly all of the error maxima in this temperature interval are located at 200 K, and without exception, errors over 10% occur only in window regions. Obviously, the root-mean-square (rms) fit error at each spectral point is much lower than the maximum error incurred. It should also be pointed out that Figure 4*a* contains results from all 16,000 spectral points and that the mean of the maximum error over the entire spectral range is less than 1%. In addition, while maximum errors for $\nu < 50{,}000$ cm^{-1} may seem prohibitively large, these errors are completely masked once allowance is made for the Herzberg contribution. This fact is evident in Figure 4*b*, where we have also plotted the magnitude of the maximum fit error for cross sections that include the underlying Herzberg continuum of *Cheung et al.* [1986*b*]. The magnitude of the Herzberg cross section is approximately 6.5×10^{-24} cm^2 within the spectral range 49,000-50,000 cm^{-1}, while minimum values for the S-R band cross section at 200 K are less than 10^{-26} cm^2 within this spectral range. For wavenumbers greater than about 51,000 cm^{-1}, the contribution by the Herzberg continuum becomes negligible compared to the S-R line wings in determining the magnitude of the cross section.

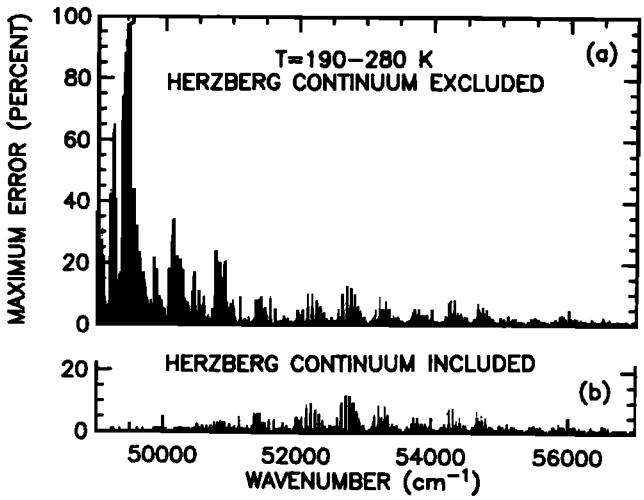

Fig. 4. Absolute value of the maximum percent error in polynomial fitted S-R cross sections over the temperature range 190-280 K. (*a*) S-R band cross sections only. Maximum errors occur near 200 K, in window regions with underlying hot lines. (*b*) Addition of the Herzberg continuum to the S-R cross sections substantially reduces the maximum fit error.

We stress that Figure 4*b* gives an indication of the maximum fit error in O_2 cross sections over the temperature range 190-280 K. For example, the 13% error at 52,738 cm^{-1} is limited to a narrow range of temperatures near 200 K, as shown in Figure 3. This error is a result of constraining the polynomial fit to match the model cross section at 190 K. Furthermore, errors of this magnitude are confined to isolated spectral points, usually at locations of hot lines. Figure 5 compares the model and polynomial-generated cross sections at 200 K, in the spectral region where the largest fit errors occur in Figure 4*b*. Deviations greater than 5% lie only at the location of 9-1 band lines, and as evidenced by the comparison at 52,738 cm^{-1} in Figure 3, the fit error is much less at other temperatures. Clearly, it is important to be cognizant of such isolated discrepancies for monochromatic, isothermal transmission calculations, but the impact of such errors is negligible for determining average transmission over a range of temperatures. The maximum and rms fit errors in the other two temperature intervals, 130-190 and 280-500 K, are also of the order of 10% and < 1%, respectively. The compound error in the polynomial-generated cross sections can be estimated from the root-sum-square error which originates from the following sources: the rms error in the polynomial fits (<1%), the mean disagreement between the line-by-line results and the laboratory measurements (~10%), and the uncertainty associated with the measurements (~5–10%). On the basis

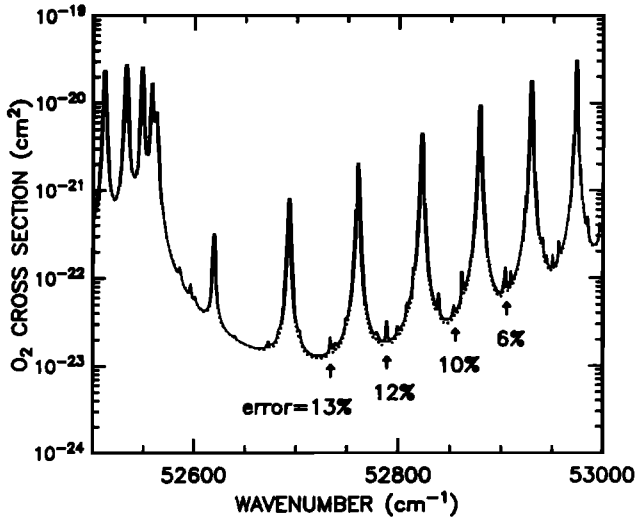

Fig. 5. Comparison of model S-R cross sections (solid) with polynomial-generated cross sections (dotted) at 200 K. It is within this spectral region, at 200 K, where the largest fit errors occur over the entire spectral range 49,000-57,000 cm^{-1}, within the temperature range 190–280 K.

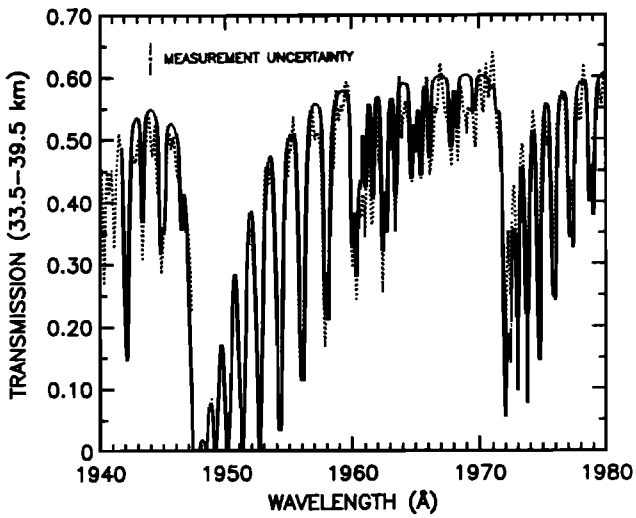

Fig. 6. Measured transmission between 39.5 and 33.5 km (dotted) by balloon-borne spectrometer [*Anderson and Hall*, 1986], along with the calculated transmission (solid) according to our polynomial-generated S-R cross sections. The 0.02-Å resolution of the calculated transmission has been degraded to 0.2 Å for comparison with the measurements. Ozone absorption is from the JPL recommended cross section [*DeMore et al.*, 1990] and the U.S. Standard Atmosphere ozone profile (1976); Rayleigh scattering is included according to cross sections given by *Goody* [1964]; and the Herzberg continuum cross section is from *Cheung et al.* [1986*b*]. The error bar represents the average error of ±0.025 which was calculated from the statistics of the measurement. The solar zenith angles are 24.8° at 39.5 km and 38.1° at 33.5 km.

of this assessment the compound error in the polynomial generated cross sections is expected to be less than 15%.

Figure 6 compares the transmission calculated with the polynomial generated cross sections to stratospheric balloon measurements [*Anderson and Hall*, 1986]. The balloon measurements have been smoothed here to provide a resolution of roughly 0.2 Å; we thus convolved the calculated transmissions with a matching 0.2-Å-wide slit function. Allowance has been made for both ozone opacity and Rayleigh scattering in the calculated transmission. The level of agreement in the optically thin case was critically dependent on values adopted for the Herzberg continuum cross section. This continuum is determined from laboratory measurements by subtracting the contribution due to the wings of S-R lines from observations taken within window regions of the spectrum. In the application of continuum values derived in this fashion to atmospheric transmission computations, it is important that the S-R wing calculations be compatible. Results of transmission calculations which employed our S-R cross sections indicated that values of the Herzberg continuum derived by *Cheung et al.* [1986*b*] provided the best agreement with the balloon observations within spectral windows.

Conversely, observations within nearly saturated line centers are difficult to obtain and may be dominated by statistical noise. In the extreme case, no information can be found if the solar irradiance at the highest measurement altitude is already blacked out. We thus conclude that the comparison is most meaningful, as far as S-R band cross sections are concerned, for transmissions > 20%, while transmissions > 50% provide a critical assessment of both S-R band and Herzberg continuum cross sections. Despite minor differences that exceed the statistical uncertainty in the measured transmission (indicated by the error bar in Figure 6), the overall level of agreement is satisfactory. We found a similar correspondence for all other spectral regions where the balloon measurements and the model cross sections overlap. The important point here is that the polynomial-generated S-R cross sections, when coupled with the appropriate Herzberg continuum, are well suited for calculating transmission at high spectral resolution.

4. CONCLUSION

The O_2 cross sections derived from our polynomial coefficients allow for an accurate representation of S-R band absorption with minimum computational expense. The approach described here cannot be guaranteed to represent the optimal method for describing the temperature dependence of S-R cross sections. Nevertheless, the polynomial coefficients derived from our line-by-line analyses constitute the most complete spectral compilation of the S-R bands currently available. We expect that the new cross sections will prove useful in reducing uncertainties surrounding S-R band transmission and photolysis rates in photochemical models of the middle atmosphere. The coefficients and implementation description are available from the NOAA World Data Center A for Solar-Terrestrial Physics, Boulder, Colorado, or from the authors.

Acknowledgments. One of the authors (K.M.) wishes to thank Steven Wofsy for extremely helpful discussions concerning the development of the Schumann-Runge line-by-line algorithm. K.M.'s research was supported by NASA grant NAGW–1230 and NSF grant ATM 89-21119 to Harvard University and by the Alexander Host Foundation. K.Y.'s work was supported by the Division of Atmospheric Science of the National Science Foundation under grant ATM-83-18960 to Harvard College Observatory. Additional funding and support was provided by the Geophysics Directorate, Phillips Laboratory, under AF contract F19628-89-C-0091 to Aerodyne Research, for the development of AURIC, the Atmospheric Ultraviolet Radiance Integrated Code.

REFERENCES

Ackerman, M., F. Biaume, and G. Kockarts, Absorption cross sections of the Schumann-Runge bands of molecular oxygen, *Planet. Space Sci., 18*, 1638–1651, 1970.

Allen, M., and J. E. Frederick, Effective photodissociation cross sections for molecular oxygen and nitric oxide in the Schumann-Runge bands, *J. Atmos. Sci., 39*, 2066–2075, 1982.

Anderson, G. P., and L. A. Hall, Stratospheric determination of O_2 cross sections and photodissociation rate coefficients: 191-215 nm, *J. Geophys. Res.*, *91*, 14,509–14,514, 1986.

Anderson, G. P., F. X. Kneizys, E. P. Shettle, L. W. Abreu, J. H. Chetwynd, R. E. Huffman, and L. A. Hall, UV spectral simulations using LOWTRAN 7, in *Atmospheric Propagation in the UV, Visible, IR and MM-Wave Region and Related Systems Aspects, AGARD-CP-454*, pp. 25-1 to 25-9, 1990.

Bass, A. M., and R. J. Paur, The ultraviolet cross sections of ozone, I, Measurements, in *Atmospheric Ozone Proceedings of the Quadrennial Ozone Symposium, Halkidiki, Greece*, edited by C. Zeferos and A. Ghazi, pp. 606–616, D. Reidel, Norwell, Mass., 1985.

Brix, P., and G. Herzberg, Fine structure of the Schumann-Runge bands near the convergence limit and the dissociation energy of the oxygen molecule, *Can. J. Phys.*, *32*, 110–135, 1954.

Cheung, A. S.-C., K. Yoshino, W. H. Parkinson, and D. E. Freeman, Molecular spectroscopic constants of $O_2(B_3\Sigma_u^-)$: The upper state of the Schumann-Runge bands, *J. Mol. Spectrosc.*, *119*, 1–10, 1986*a*.

Cheung, A. S.-C., K. Yoshino, W. H. Parkinson, S. L. Guberman, and D. E. Freeman, Absorption cross section measurements of oxygen in the wavelength region 195-241 nm of the Herzberg continuum, *Planet. Space Sci.*, *34*, 1007–1016, 1986*b*.

Cheung, A. S.-C., K. Yoshino, D. E. Freeman, R. S. Friedman, A. Dalgarno, and W. H. Parkinson, The Schumann-Runge bands of $^{16}O^{18}O$ in the wavelength region 175-205 nm and the spectroscopic constants of isotopic oxygen molecules, *J. Mol. Spectrosc.*, *134*, 362–389, 1989.

Cheung, A. S.-C., K. Yoshino, J. R. Esmond, S. S-L Chiu, D. E. Freeman, and W. H. Parkinson, Predissociation line widths of the (1,0) - (12,0) Schumann-Runge absorption bands of O_2 in the wavelength region 179-202 nm, *J. Chem. Phys.*, *92*, 842–849, 1990.

Chiu, S. S.-L., A. S.-C. Cheung, K. Yoshino, J. R. Esmond, D. E Freeman, and W. H. Parkinson, Predissociation line widths of the (3,0)-(11,0) Schumann-Runge absorption bands of $^{18}O_2$ and $^{16}O^{18}O$ in the wavelength region 180-196 nm, *J. Chem. Phys.*, *93*,, 5539–5543, 1990.

DeMore, W. B., S. P. Sander, D. M. Golden, M. J. Molina, R. F. Hampson, M. J. Kurylo, C. J. Howard, and A. R. Ravishankara, Chemical kinetics and photochemical data for use in stratospheric modeling, Evaluation 9, *JPL Publ. 90–1*, 217, 1990.

Drayson, S. R., Rapid computation of the Voigt profile, *J. Quant. Spectrosc. Radiat. Transfer*, *16*, 611–614, 1976.

Fang, T. M., S. C. Wofsy, and A. Dalgarno, Opacity distribution functions and absorption in the Schumann-Runge bands of molecular oxygen, *Planet. Space Sci.*, *22*, 413–425, 1974.

Goody, R. M., *Atmospheric Radiation: Theoretical Basis*, Appendix 12, Oxford University Press, New York, 1964.

Hudson, R. D., and V. L. Carter, Absorption of oxygen at elevated temperatures (300 to 900 K) in the Schumann-Runge system, *J. Opt. Sci. Am.*, *58*, 1621–1629, 1968.

Kneizys, F. X., E. P. Shettle, L. W. Abreu, J. H. Chetwynd, G. P. Anderson, W. O. Gallery, J. E. A. Selby, and S. A. Clough, Users guide to LOWTRAN 7, *AFGL-TR-88-0177, AD A206773*, 137, 1988.

Lewis, B. R., L. Berzins, and J. H. Carver, Decomposition of the photoabsorption continuum underlying the Schumann-Runge bands of $^{16}O_2$, I, Role of the $B^3\Sigma_u^-$ state: A new dissociation limit, *J. Quant. Spectrosc. Radiat. Transfer*, *33*, 627–643, 1985*a*.

Lewis, B. R., L. Berzins, and J. H. Carver, Decomposition of the photoabsorption continuum underlying the Schumann-Runge bands of $^{16}O_2$, II, Role of the $1\,^3\Pi_g$ state and collision-induced absorption, *J. Quant. Spectrosc. Radiat. Transfer*, *34*, 405–415, 1985*b*.

Lewis, B. R., L. Berzins, and J. H. Carver, Oscillator strengths for the Schumann-Runge bands of O_2, *J. Quant. Spectrosc. Radiat. Transfer*, *36*, 209–232, 1986*a*.

Lewis, B. R., L. Berzins, J. H. Carver, and S. T. Gibson, Rotational variation of predissociation linewidth in the Schumann-Runge bands of $^{16}O_2$, *J. Quant. Spectrosc. Radiat. Transfer*, *36*, 187–207, 1986*b*.

Murtagh, D. P., The O_2 Schumann-Runge system: New calculations of photodissociation cross sections, *Planet. Space. Sci.*, *36*, 819–828, 1988.

Nicolet, M., and R. Kennes, Aeronomic problems of the molecular oxygen photodissociation, I, The O_2 Herzberg continuum, *Planet. Space Sci.*, *11*, 1043–1059, 1986.

Nicolet, M., and R. Kennes, Aeronomic problems of molecular oxygen photodissociation, IV, Photodissociation frequency and transmittance in the spectral range of the Schumann-Runge bands, *Planet. Space Sci.*, *37*, 459–491, 1989.

Nicolet, M., and W. Peetermans, Atmospheric absorption in the O_2 Schumann-Runge band spectral range and photodissociation rates in the stratosphere and mesosphere, *Planet. Space Sci.*, *28*, 85–103, 1980.

Park, J. H., The equivalent mean absorption cross sections for the O_2 Schumann-Runge bands: Application to the H_2O and NO photodissociation rates, *J. Atmos. Sci.*, *31*, 1893–1897, 1974.

Tatum, J. B., and J. K. G. Watson, Rotational line strengths in $3(\Sigma)$-$3(\Sigma)$ transitions with intermediate coupling, *Can. J. Phys.*, *49*, 2693–2703, 1971.

Veseth, L., and A. Lofthus, Fine structure and centrifugal distortion in the electronic and microwave spectra of O_2 and SO, *Mol. Phys.*, *27*, 511–519, 1974.

World Meteorological Organization, (WMO) Global ozone research and monitoring project, Report 16, Atmospheric Ozone 1985: Assessment of Our Understanding of the Processes Controlling Its Present Distribution and Change, Geneva, Switzerland, 1986.

Yoshino, K., D. E. Freeman, J. R. Esmond, and W. H. Parkinson, High resolution absorption cross section measurements and band oscillator strengths of the (1,0)-(12,0) Schumann-Runge bands of O_2, *Planet. Space Sci.*, *31*, 339–353, 1983.

Yoshino, K., D. E. Freeman, J. R. Esmond, and W. H. Parkinson, High resolution absorption cross sections and band oscillator strengths of the Schumann-Runge bands of oxygen at 79 K, *Planet. Space Sci.*, *35*, 1067–1075, 1987.

Yoshino, K., A. S.-C. Cheung, J. R. Esmond, W. H. Parkinson, D. E. Freeman, and S. L. Guberman, Improved absorption cross sections of oxygen in the wavelength region 205-240 nm of the Herzberg continuum, *Planet. Space Sci.*, *36*, 1469–1475, 1988.

Yoshino, K., D. E. Freeman, J. R. Esmond, R. S. Friedman, and W. H. Parkinson, High resolution absorption cross sections and band oscillator strengths of the Schumann-Runge absorption bands of isotopic oxygen, $^{16}O^{18}O$, at 79 K, *Planet. Space Sci.*, *37*, 419–426, 1989.

Yoshino, K., J. R. Esmond, A. S.-C. Cheung, D. E. Freeman, and W. H. Parkinson, High resolution absorption cross sections in the transmission window region of the Schumann-Runge bands and Herzberg continuum of O_2, *Planet. Space Sci. 40*, 185–192, 1992.

G. P. Anderson, Geophysics Directorate, Phillips Laboratory/GPOS, Hanscom AFB, MA 01731.

L. A. Hall, Geophysics Directorate, Phillips Laboratory/GPIM, Hanscom AFB, MA 01731.

K. Minschwaner, Department of Earth and Planetary Sciences, Harvard University, Cambridge, MA 02138.

K. Yoshino, Harvard-Smithsonian Center for Astrophysics, Cambridge, MA 02138.

(Received November 25, 1991;
revised March 16, 1992;
accepted March 16, 1992.)